

Pricing the financial Heston–Hull–White model with arbitrary correlation factors via an adaptive FDM

Fazlollah Soleymani*, Behzad Nemati Saray

Department of Mathematics, Institute for Advanced Studies in Basic Sciences (IASBS), Zanjan 45137-66731, Iran



ARTICLE INFO

Article history:

Received 23 June 2018

Received in revised form 14 October 2018

Accepted 28 October 2018

Available online 16 November 2018

Keywords:

Option pricing

Stochastic interest rate

Heston–Hull–White model

Discontinuity

PDE

ABSTRACT

This paper is concerned with the pricing procedure of one of the most challenging models known as the Heston–Hull–White partial differential equation (PDE) in option pricing, at which the model is a time-dependent 3D linear PDE including three mixed derivative terms. The model comes from the fact that the price, the volatility and the interest rate are assumed to be stochastic processes. To contribute and avoid huge discretized systems, an adaptive distribution of the nodes (viz, nonuniform nodes) is taken into account with emphasis on the hot area of the solution curve. New adaptive finite difference (FD) formulas of higher orders are constructed on these meshes. Then, a set of semi-discretized equations is attained which is tackled by a time-stepping method. Several financial tests are discussed in detail to reveal the superiority of the proposed approach.

© 2018 Elsevier Ltd. All rights reserved.

1. Introductory notes

Option pricing is one of the important problems of financial engineering, [1]. Today financial assets (stocks, bonds, commodities, etc.) are used as a base for thousands of more complex financial products known as financial derivatives. To tackle such problems, there are three important classes of computational methods in financial engineering: Monte-Carlo methods, tree-based methods and deterministic methods based on a PDE. The objective of the present work is to focus on the latter, see, e.g., [2,3].

This paper is concerned with the option valuation of European-style options under the challenging model of Heston–Hull–White. In foreign exchange markets, option pricing with stochastic volatility and stochastic interest rates has received a good amount of interest in the last few years leading to the extension of the Heston two-factor stochastic volatility model [4] and the Schöbel–Zhu model to currency derivatives [5].

Although appealing due to its simplicity, assuming constant interest rates is inappropriate for long-dated foreign exchange products, and the effect of interest rate volatility can even outweigh that of foreign exchange rate volatility for long maturities, which is the fact discussed deeply in [6].

In the pioneer work [7], it was discussed and considered that in order to price the real data from the market as accurately as possible, the interest must be taken into consideration as a stochastic process, which would yield to the well-known CIR model. This assumption generalizes the idea of the Black–Scholes theory, at which the interest rate is constant. Further discussions about stochastic interest rates might be read in [8,9].

Apart from [7], Hull and White in another seminal work [10] revealed another way for introducing the stochastically behavior of the interest rate into a model using stochastic differential equations (SDEs) in order to model real-world cases of

* Corresponding author.

E-mail addresses: soleymani@iasbs.ac.ir, fazl_soley_bsb@yahoo.com (F. Soleymani), bn.saray@iasbs.ac.ir (B.N. Saray).

the market. In fact, the work [10] presented a trinomial tree-building procedure for implementing one-factor no-arbitrage models of the short rate. The key assumption is that a function, $f(r)$, of the short rate, r , follows an Ornstein–Uhlenbeck process with a reversion level that is a function of time, see for more [11]. One-factor no-arbitrage models of the short rate have a number of applications in finance. For example, they can be used to value non-standard interest rate derivatives such as Bermudan swap options.

Pricing the derivatives using the CIR model are possible when the interest rate is (theoretically) changing in $[0, +\infty)$, while in the Hull–White model for pricing the financial derivatives, the interest rate is (theoretically) changing $(-\infty, +\infty)$.

Authors in [12] discussed that the consideration of constant interest rates in the Black–Scholes model can be extended, whereas by including the stochastic interest rate process of [10], an exact solution can be attained for European-style option prices.

The two models which take both volatility and interest rates to be as stochastic processes, i.e., the Heston–Hull–White (HHW) hybrid model and the Heston–Cox–Ingersoll–Ross (HCIR) hybrid model, were discussed in [13]. In fact, authors proposed approximations such that the characteristic functions of the SDE models can be attained while it does not require the preliminary calculations of expectations.

These models are unable to produce the interest rate implied volatility smiles or skews. Accordingly, their main applications concentrate on long-term equity options and for equity-interest rate hybrid products. For a complete background and further literature regarding this option pricing problem, one may refer to the works [14–16].

The necessity of considering and developing models based on stochastic interest rates have been considered in several practical works. However, the literature on this subject (in terms of numerical methods) includes Fourier–Cosine methods, semi-closed approximations and finite-difference methods (FDMs) to price vanilla options. As an illustration, authors in [6] extended and proposed a stochastic volatility model to equity and currency derivatives via considering stochastic interest rates and taking into consideration that all driving model factors to be correlated spontaneously.

An interest rate model using Gaussian notion was also used in [17], whereas a local volatility model was discussed to produce the existing skews in the foreign exchange market. The HHW model with the interest rate as a stochastic process was treated using semi-closed approximations in the foreign exchange model [18].

Recently in [2], the hybrid tree method along with FD approach was discussed and applied for HHW (SDE) model by writing down an algorithm for option pricing via a backward induction which works following an FDM in the direction of the share process and following a recombining binomial tree method in the direction of the other random sources (the volatility, and the interest rate). Furthermore, they applied a new Monte Carlo algorithm which, is an extension over the standard Monte Carlo algorithm.

In general, pricing in the category of HCIR and HHW models should be pursued computationally, since they do not admit any closed-form solutions. In this work, we focus on a general PDE model due to the HHW model and call it a 3D HHW PDE for option pricing when not only the stock price, but also the volatility and the interest rate are stochastic processes.

In [19], the authors discussed how to price European call options and also double barrier knock-out call options via an adaption of computational nodes based on a 3D financial HHW PDE. The method discussed is not computationally fast although the computational nodes are taken to be adaptive, since the convergence rate of the approximations are only one for the 2nd derivative and of second order for the 1st derivative terms involving in the PDE-based model.

It is clearly pointed out that throughout the paper, adaptive means a nonuniform discretizations of the nodes with a clear emphasis on the hot area, at which the solution is non-differentiable, degenerate and required.

Our goal is to derive a computationally fast scheme for pricing European options under the fact that asset price and also the volatility and the interest rate all coming from stochastic processes. Note that the rate of fair pricing European products is of importance for the calibration. Accordingly, we aim at proposing a fast and reliable algorithm for this problem.

To contribute, the financial 3D model is semi-discretized (see [20,21] for background) along the spatial variables using adaptive distribution of the nodes via *new adaptive higher-order* FD approximations. Following this procedure, we obtain a set of Ordinary Differential Equations (ODEs) subject to an initial condition, which can effectively be calculated by applying a simple-to-implement time-stepping solver.

For the final fully-discretized scheme, it is discussed that the overall computational procedure is conditionally stable. Since symbolic and numerical codings are necessary all at the same time, the implementations are done in the recent versions of Mathematica. Another important advantage of using this programming package occurs when imposing the boundary conditions for this 3D challenging PDE problem. Note that for one face of the computational domain, no boundary condition should be imposed due to encountering with degeneracy [19].

This work is organized in what follows. In Section 2, the HHW model as a system of SDEs and its corresponding PDE form as a 3D time-dependent second-order PDE under a non-smooth initial condition for pricing are introduced and formulated. In Section 3, a computational grid of nodes is described which has a clear concentration around the hotzone to increase the accuracy of the computed prices for this model. Section 4 is devoted to presenting a fast and high-order adaptive FD formula for semi-discretization of the model.

Then in Section 5, the method-of-lines approach is taken into account to construct a system of ODEs with varying coefficient matrix. Boundary conditions are significant in order to guarantee reaching a desired solution curve which exist and unique. Thus, in Section 6, these conditions are introduced and discussed. A time-stepping solver for the ODE part is given and implemented in Section 7. Section 8 compares the applicability and efficiency of our new adaptive FDM with the well-known schemes in the literature. Ultimately, Section 9 offers a conclusion and an outline for future researches.

2. Modeling framework

The dynamic of the classical Heston model under the risk-neutral pricing measure with the variance process $V(\tau)$ and the stock $S(\tau)$, is defined as follows [4]:

$$\begin{aligned} \frac{dS(\tau)}{S(\tau)} &= rd\tau + \sqrt{V(\tau)}dW_1(\tau), & S(\tau) > 0, \\ dV(\tau) &= \kappa(\eta - V(\tau))d\tau + \gamma\sqrt{V(\tau)}dW_2(\tau), & V(\tau) > 0, \end{aligned} \quad (1)$$

wherein $r > 0$ is the constant risk-free interest rate, correlation $dW_1(\tau)dW_2(\tau) = \rho dt$, and $X(\tau) = (S(\tau), V(\tau))^*$ is the state vector. Here $v(\tau)$ is a mean reverting square-root process, whereas $\kappa > 0$ specifies the speed of adjustment of the volatility towards its theoretical mean $\eta > 0$. Noting that $\gamma > 0$ is the second-order volatility, i.e., the volatility of volatility.

The HHW model [13] as a system of three SDEs is defined as:

$$\begin{aligned} dS(\tau) &= R(\tau)S(\tau)d\tau + \sqrt{V(\tau)}S(\tau)dW_1(\tau), \\ dV(\tau) &= \kappa(\eta - V(\tau))d\tau + \sigma_1\sqrt{V(\tau)}dW_2(\tau), \\ dR(\tau) &= a(b(\tau) - R(\tau))d\tau + \sigma_2dW_3(\tau), \end{aligned} \quad (2)$$

whereas $S(\tau)$, $V(\tau)$, and $R(\tau)$ are three random variables to represent the asset price, its variance and the interest rate, respectively, at time $0 < \tau \leq T$. In (2), b is a given and positive function of time, which is called the mean-reversion level. Here the parameters κ , η , σ_1 , σ_2 , a are positive real constants while $W_1(\tau)$, $W_2(\tau)$, $W_3(\tau)$ are Brownian motions under a risk-neutral measure. The correlation parameters for these Brownian motions are $\rho_{12}, \rho_{13}, \rho_{23} \in [-1, 1]$.

The risk-neutral value for a European option pricing problem using the dynamics in (2) is defined in what follows [13]:

$$\varphi(s, v, r, \tau) = \mathbb{E} \left[\exp \left(- \int_{\tau}^T R(\varsigma)d\varsigma \right) \phi(S(T), V(T), R(T)) \middle| S(\tau) = s, V(\tau) = v, R(\tau) = r \right], \quad (3)$$

wherein T , s , v , and r , are the maturity time, the asset price, the variance, and the interest rate, respectively. Here \mathbb{E} is the conditional expectation and ϕ is the payoff function. Taking into account that the pricing function reads

$$u(s, v, r, t) = \varphi(s, v, r, T - t), \quad (4)$$

then the option pricing problem as a PDE-model is given as follows:

$$\begin{aligned} \frac{\partial u(s, v, r, t)}{\partial t} &= \frac{1}{2}s^2v\frac{\partial^2 u(s, v, r, t)}{\partial s^2} + \frac{1}{2}\sigma_1^2v\frac{\partial^2 u(s, v, r, t)}{\partial v^2} + \frac{1}{2}\sigma_2^2\frac{\partial^2 u(s, v, r, t)}{\partial r^2} \\ &\quad + \rho_{12}\sigma_1sv\frac{\partial^2 u(s, v, r, t)}{\partial s \partial v} + \rho_{13}\sigma_2s\sqrt{v}\frac{\partial^2 u(s, v, r, t)}{\partial s \partial r} + \rho_{23}\sigma_1\sigma_2\sqrt{v}\frac{\partial^2 u(s, v, r, t)}{\partial v \partial r} \\ &\quad + rs\frac{\partial u(s, v, r, t)}{\partial s} + \kappa(\eta - v)\frac{\partial u(s, v, r, t)}{\partial v} + a(b(T - t) - r)\frac{\partial u(s, v, r, t)}{\partial r} \\ &\quad - ru(s, v, r, t), \end{aligned} \quad (5)$$

where u is sufficiently smooth. The 3D financial PDE problem (5) consists of three mixed derivative terms originating from the correlation among the asset price, and its variance and the interest rate. The diffusion matrix corresponds to (5) is given by:

$$D(s, v) = \frac{1}{2} \begin{pmatrix} s^2v & \rho_{12}\sigma_1sv & \rho_{13}\sigma_2s\sqrt{v} \\ \rho_{12}\sigma_1sv & \sigma_1^2v & \rho_{23}\sigma_1\sigma_2\sqrt{v} \\ \rho_{13}\sigma_2s\sqrt{v} & \rho_{23}\sigma_1\sigma_2\sqrt{v} & \sigma_2^2 \end{pmatrix}. \quad (6)$$

For call options in the HHW PDE problem (5), the initial condition is furnished by the following payoff function

$$u(s, v, r, 0) = \phi(s, v, r) = \max\{0, s - E\}, \quad (7)$$

where E is the strike price.

The PDE model (5) is a parabolic PDE on the following unbounded domain: $(s, v, r, t) \in [0, +\infty) \times [0, +\infty) \times (-\infty, +\infty) \times (0, T]$. Herein, the HHW model can take any positive or negative values for the interest rate r . Moreover, the coefficient of $\frac{\partial u(s, v, r, t)}{\partial r}$ is time-dependent.

To tackle the model computationally, we should localize it into a bounded computational domain. Since the problem is well-posed and a viscosity solution exists [22, page 336], the computational domain can be considered to be bounded as follows:

$$(s, v, r, t) \in [0, s_{\max}] \times [0, v_{\max}] \times [-r_{\max}, r_{\max}] \times (0, T], \quad (8)$$

wherein s_{\max} , v_{\max} , r_{\max} are three positive real constant considered large enough so as to minimize the error of the domain truncation.

It is not clear where to place s_{\max} , v_{\max} , and r_{\max} , precisely. Subsequently, it is required to place them far away. This reduces the error of the artificial boundary conditions but contributes in the fact that a large computational domain requires a large discretization width. Accordingly, this increases the error of the approximation of the derivatives. Thus, an adaptive distribution of the nodes for such problems are the only remedy in order to tackle the problem as efficiently as possible. This would be discussed in Section 3.

The HHW PDE as an initial-boundary value problem does not admit any theoretical or analytic solution in closed form. This shifts the focus on the numerically fast algorithms for tackling this challenging 3D problem. However, it is recalled that authors in [19] provided an analytic solution for (5) under strict conditions for the correlation factors to satisfy

$$\rho_{13} = \rho_{23} = 0, \quad (9)$$

and an extension of the Heston approach given in [4].

Since the diffusion part of (5) has a clear effect on the accuracy of the computational pricing solution, so the main aim here is to propose adaptive FD formulas of higher orders, i.e., second order of convergence for the diffusion terms and third order of convergence for the convection terms.

3. Meshing

The efficient generation of meshes is an important component in the numerical solution of problems in finance. In fact, the computational solution of time-dependent financial PDEs may require the use of a mesh refinement strategy that concentrates more mesh points where the solution and/or its derivatives change rapidly or is non-differentiable, i.e., at the hot zone in our problem (5).

Let $\{s_i\}_{i=1}^m$ be a partition along the spatial variable $s \in [s_{\min}, s_{\max}]$. Then, the meshing along this variable is defined as follows [19]:

$$s_i = \mathcal{E}(\xi_i), \quad 1 \leq i \leq m, \quad (10)$$

wherein $m > 1$ is an integer defining the number of points along with the s -axis and $\xi_{\min} = \xi_1 < \xi_2 < \dots < \xi_m = \xi_{\max}$ are m uniform nodes with the following specifications:

$$\begin{aligned} \xi_{\min} &= \sinh^{-1} \left(\frac{s_{\min} - s_{\text{left}}}{d_1} \right), \\ \xi_{\text{int}} &= \frac{s_{\text{right}} - s_{\text{left}}}{d_1}, \\ \xi_{\max} &= \xi_{\text{int}} + \sinh^{-1} \left(\frac{s_{\max} - s_{\text{right}}}{d_1} \right), \end{aligned} \quad (11)$$

wherein $s_{\min} = 0$. Here $\sinh^{-1}(\cdot)$ stands for the inverse hyperbolic sine function. Note that the parameter $d_1 > 0$ is a constant that conducts the fraction of the mesh nodes s_i that are situated around $s = E$. Here the zoom function is defined by:

$$\mathcal{E}(\xi) = \begin{cases} s_{\text{left}} + d_1 \sinh(\xi), & \xi_{\min} \leq \xi < 0, \\ s_{\text{left}} + d_1 \xi, & 0 \leq \xi \leq \xi_{\text{int}}, \\ s_{\text{right}} + d_1 \sinh(\xi - \xi_{\text{int}}), & \xi_{\text{int}} < \xi \leq \xi_{\max}. \end{cases} \quad (12)$$

In implementations, we used the value $d_1 = \frac{E}{20}$, while $s_{\text{left}} = \max\{0.5, \exp\{-0.25T\}\} \times E$, $s_{\text{right}} = E$, $[s_{\text{left}}, s_{\text{right}}] \subset [0, s_{\max}]$, and $s_{\max} = 1400$.

In a similar manner, if $\{v_j\}_{j=1}^n$ stands for a partition along the spatial variable v , then the meshing in this direction which should be focused around zero (from the right side) could be defined as follows:

$$v_j = d_2 \sinh(\zeta_j), \quad 1 \leq j \leq n, \quad (13)$$

wherein $n > 1$ is an integer defining the number of nodes along the variable $v \in [0, v_{\max}]$, $d_2 > 0$ is a constant that controls the fraction of the mesh points v_j that lie near $v = 0$. In implementations, we used $d_2 = \frac{v_{\max}}{500}$, whereas $v_{\max} = 10$. Furthermore, here ζ_j are equidistant points given by

$$\zeta_j = (j - 1)\Delta\zeta, \quad \Delta\zeta = \frac{1}{n - 1} \sinh^{-1} \left(\frac{v_{\max}}{d_2} \right), \quad (14)$$

for any $1 \leq j \leq n$. The discretization in the third spatial direction, $r \in [-r_{\max}, r_{\max}]$, is done in what follows:

$$r_k = c + d_3 \sinh(\xi_k), \quad 1 \leq k \leq o, \quad (15)$$

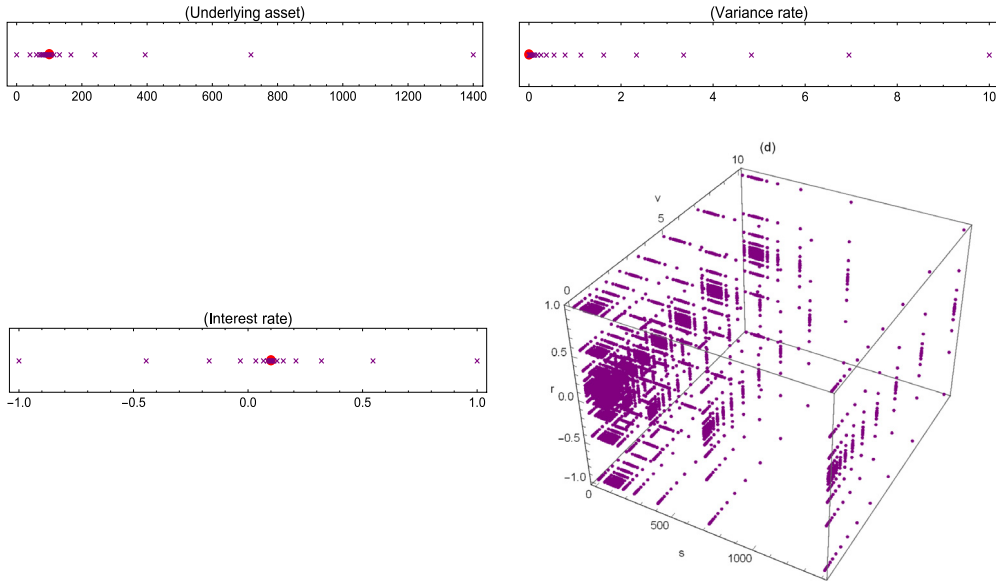


Fig. 1. The adaptive distribution of the nodes for $m = 20$, $n = 20$ and $o = 20$, along s in (underlying asset), along v in (variance rate), along r in (interest rate) and for the 3D computational domain in (d). The hot area is shown by a red point.

whereas $d_3 = \frac{r_{\max}}{400}$ is a positive parameter that controls the density of the computational nodes around $r = c$, while $r_{\max} = 1$. In this case, we have

$$\xi_k = \sinh^{-1} \left(\frac{-r_{\max} - c}{d_3} \right) + (k - 1)\Delta\xi, \quad (16)$$

where

$$\Delta\xi = \frac{1}{o - 1} \left[\sinh^{-1} \left(\frac{r_{\max} - c}{d_3} \right) - \sinh^{-1} \left(\frac{-r_{\max} - c}{d_3} \right) \right]. \quad (17)$$

The parameters d_1 , d_2 and d_3 are chosen so as to focus on the hot area as much as possible, while avoiding from ill-conditioned matrices when high number of discretization nodes are considered. The final adaptive computational grid with a clear concentration around the hotzone is attained using a Cartesian product of the grids along s by (10), v by (13) and r by (15) in what follows:

$$\text{Computational grid} = \{s_i\} \times \{v_j\} \times \{r_k\}, \quad 1 \leq i \leq m, 1 \leq j \leq n, 1 \leq k \leq o. \quad (18)$$

The concentration of computational nodes using (18) are around the hotzone, $(s, v, r) = (E, 0, c)$. An illustration for such a grid is brought forward in Fig. 1 for the case $m = n = o = 20$, and $c = 0.1$.

4. High-order adaptive approximations

In practice, the approximation for the convection and the diffusion terms of (5) are all of importance. However, when dealing with high-dimensional PDEs, it is necessary to propose computational methods, which provide sparse formulas in order to avoid handling very large scale dense matrices.

Accordingly, in this section adaptive FD formulas are constructed (based on the logic introduced in [23, chapters 3–4]) to achieve several aspects at the same time, i.e., to be efficient, yields sparse matrices and could be performed on the adaptive grid of points (10), (13) and (15). To keep the sparsity as high as possible, while to keep the convergence order as high as possible, only four adjacent computational nodes which are not equidistant are considered for finding the FD approximations along each spatial variable, i.e., the asset price, its variance and its interest rate. Following such an approach, the convergence speeds for the convection and diffusion approximations would be three and two, respectively. These are higher than the existing adaptive FD formulas for this aim, which are second order for the convection and first order for the diffusion terms previously presented in [19].

Without loss of generality, consider a general setting for a one-dimensional sufficiently smooth function $f(x)$ and a smooth non-uniform grid given as $\{x_1, x_2, \dots, x_{m-1}, x_m\}$. To approximate the first derivative in a non-uniform grid for the interior nodes by applying the following four nodes $\{(x_{i-2}, f(x_{i-2})), (x_{i-1}, f(x_{i-1})), (x_i, f(x_i)), (x_{i+1}, f(x_{i+1}))\}$, where $3 \leq i \leq m - 2$,

first we obtain an interpolating polynomial passing through these adjacent nodes, and then its first derivative as follows:

$$\begin{aligned} p'(z) = & \frac{1}{\Delta_{i-2,i-1}\Delta_{i-2,i}\Delta_{i-2,i+1}\Delta_{i-1,i}\Delta_{i-1,i+1}\Delta_{i,i+1}} \\ & \times (\Delta_{i-2,i-1}\Delta_{i-2,i}\Delta_{i-1,i}(-f(x_{i+1}))(x_{i-1}(x_i - 2z) + x_{i-2}(x_{i-1} + x_i - 2z) + z(3z - 2x_i))) \\ & + \Delta_{i-2,i-1}\Delta_{i-2,i+1}\Delta_{i-1,i+1} + f(x_i)(x_{i-1}(x_{i+1} - 2z) + x_{i-2}(x_{i-1} + x_{i+1} - 2z) + z(3z - 2x_{i+1})) \\ & - ((\Delta_{i-2,i}\Delta_{i-2,i+1}f(x_{i-1})(x_i(x_{i+1} - 2z) + x_{i-2}(x_i + x_{i+1} - 2z) + z(3z - 2x_{i+1}))) \\ & + \Delta_{i-1,i}\Delta_{i-1,i+1}(-f(x_{i-2}))(x_i(x_{i+1} - 2z) + x_{i-1}(x_i + x_{i+1} - 2z) + z(3z - 2x_{i+1})))\Delta_{i,i+1}). \end{aligned} \quad (19)$$

Setting $z = x_i$ in (19), and some simplifications, we obtain the following FD formula for the first derivative

$$\begin{aligned} f'(x_i) = & -\frac{\Delta_{i-1,i}\Delta_{i,i+1}}{\Delta_{i-2,i-1}\Delta_{i-2,i}\Delta_{i-2,i+1}}f(x_{i-2}) + \frac{\Delta_{i-2,i}\Delta_{i,i+1}}{\Delta_{i-2,i-1}\Delta_{i-1,i}\Delta_{i-1,i+1}}f(x_{i-1}) \\ & + \left(\frac{1}{\Delta_{i,i-1}} + \frac{1}{\Delta_{i,i+1}} + \frac{1}{\Delta_{i,i-2}}\right)f(x_i) + \frac{\Delta_{i-2,i}\Delta_{i,i-1}}{\Delta_{i-2,i+1}\Delta_{i+1,i-1}\Delta_{i+1,i}}f(x_{i+1}) \\ & + \mathcal{O}(h^3). \end{aligned} \quad (20)$$

wherein h is the maximum local grid spacing and $\Delta_{l,q} = x_l - x_q$. For the nodes x_1 and x_2 and using $\{(x_1, f(x_1)), (x_2, f(x_2)), (x_3, f(x_3)), (x_4, f(x_4))\}$, we obtain

$$\begin{aligned} f'(x_1) = & \left(\frac{1}{\Delta_{1,3}} + \frac{1}{\Delta_{1,4}} + \frac{1}{\Delta_{1,2}}\right)f(x_1) - \frac{\Delta_{1,3}\Delta_{1,4}}{\Delta_{2,4}\Delta_{1,2}\Delta_{2,3}}f(x_2) \\ & - \frac{\Delta_{1,2}\Delta_{1,4}}{\Delta_{1,3}\Delta_{3,2}\Delta_{3,4}}f(x_3) - \frac{\Delta_{1,2}\Delta_{1,3}}{\Delta_{1,4}\Delta_{4,2}\Delta_{4,3}}f(x_4) \\ & + \mathcal{O}(h^3), \end{aligned} \quad (21)$$

and

$$\begin{aligned} f'(x_2) = & \frac{\Delta_{2,3}\Delta_{2,4}}{\Delta_{1,2}\Delta_{1,3}\Delta_{1,4}}f(x_1) + \left(\frac{1}{\Delta_{2,3}} + \frac{1}{\Delta_{2,4}} + \frac{1}{\Delta_{2,1}}\right)f(x_2) \\ & + \frac{\Delta_{1,2}\Delta_{2,4}}{\Delta_{1,3}\Delta_{3,2}\Delta_{3,4}}f(x_3) + \frac{\Delta_{1,2}\Delta_{2,3}}{\Delta_{1,4}\Delta_{4,2}\Delta_{4,3}}f(x_4) \\ & + \mathcal{O}(h^3). \end{aligned} \quad (22)$$

Now by using $\{(x_m, f(x_m)), (x_{m-1}, f(x_{m-1})), (x_{m-2}, f(x_{m-2})), (x_{m-3}, f(x_{m-3}))\}$, we can find the third-order FD formulas in the last two nodes x_{m-1}, x_m in what follows:

$$\begin{aligned} f'(x_{m-1}) = & \frac{\Delta_{m-3,m-1}\Delta_{m-1,m-2}}{\Delta_{m-3,m}\Delta_{m,m-2}\Delta_{m,m-1}}f(x_m) + \left(\frac{1}{\Delta_{m-1,m-2}} + \frac{1}{\Delta_{m-1,m}} + \frac{1}{\Delta_{m-1,m-3}}\right)f(x_{m-1}) \\ & + \frac{\Delta_{m-3,m-1}\Delta_{m-1,m}}{\Delta_{m-3,m-2}\Delta_{m-2,m-1}\Delta_{m-2,m}}f(x_{m-2}) - \frac{\Delta_{m-2,m-1}\Delta_{m-1,m}}{\Delta_{m-3,m-2}\Delta_{m-3,m-1}\Delta_{m-3,m}}f(x_{m-3}) \\ & + \mathcal{O}(h^3), \end{aligned} \quad (23)$$

and

$$\begin{aligned} f'(x_m) = & \left(\frac{1}{\Delta_{m,m-2}} + \frac{1}{\Delta_{m,m-1}} + \frac{1}{\Delta_{m,m-3}}\right)f(x_m) + \frac{\Delta_{m-3,m}\Delta_{m,m-2}}{\Delta_{m-3,m-1}\Delta_{m-1,m-2}\Delta_{m-1,m}}f(x_{m-1}) \\ & + \frac{\Delta_{m-3,m}\Delta_{m,m-1}}{\Delta_{m-3,m-2}\Delta_{m-2,m-1}\Delta_{m-2,m}}f(x_{m-2}) + \frac{\Delta_{m-2,m}\Delta_{m-1,m}}{\Delta_{m-3,m-2}\Delta_{m-3,m-1}\Delta_{m-3,m}}f(x_{m-3}) \\ & + \mathcal{O}(h^3). \end{aligned} \quad (24)$$

Since for nonzero correlations, the PDE (5) includes exactly three mixed spatial-derivative terms. We could compute the FD formulas of these terms based on (20)–(24). Let $f : \mathbb{R}^2 \rightarrow \mathbb{R}$ be a given real function including two variables (x, y) , then the cross derivative

$$\frac{\partial^2 f}{\partial x \partial y} = \frac{\partial}{\partial x} \left(\frac{\partial}{\partial y} \right) f, \quad (25)$$

is approximated at any point (x_i, y_j) by the successive application of the FD formulas (20)–(24) in the x - and y -directions. For multi-dimensional derivatives, a matrix is constructed such that this is done on the flattened data, and subsequently the Kronecker product (denoted by \otimes) of the matrices for the derivatives (in one-dimension) are being considered.

In the same vein, FD formulas for the diffusion-term may be attained using a similar strategy as in the convection-term approximating. Toward this goal, the following set of interior nodes (here $3 \leq i \leq m-2$) are considered: $\{(x_{i-2}, f(x_{i-2}))$,

$\{x_{i-1}, f(x_{i-1})\}, \{x_i, f(x_i)\}, \{x_{i+1}, f(x_{i+1})\}$, then we obtain the following second-derivative of the interpolation polynomial in terms of z :

$$\begin{aligned} p''(z) = & \frac{1}{\Delta_{i-2,i-1}\Delta_{i-2,i}\Delta_{i-2,i+1}\Delta_{i-1,i}\Delta_{i-1,i+1}\Delta_{i,i+1}} \\ & \times 2(\Delta_{i-2,i-1}\Delta_{i-2,i}\Delta_{i-1,i}f(x_{i+1})(x_{i-2} + x_{i-1} + x_i - 3z) \\ & + \Delta_{i-2,i-1}\Delta_{i-2,i+1}\Delta_{i-1,i+1}(-f(x_i))(x_{i-2} + x_{i-1} + x_{i+1} - 3z) \\ & + (\Delta_{i-2,i}\Delta_{i-2,i+1}f(x_{i-1})(x_{i-2} + x_i + x_{i+1} - 3z) \\ & + \Delta_{i-1,i}\Delta_{i-1,i+1}(-f(x_{i-2}))(x_{i-1} + x_i + x_{i+1} - 3z))\Delta_{i,i+1}. \end{aligned} \quad (26)$$

Setting $z = x_i$, we have

$$\begin{aligned} f''(x_i) = & \frac{2(\Delta_{i-1,i} + \Delta_{i+1,i})}{\Delta_{i-1,i-2}\Delta_{i-2,i}\Delta_{i+1,i-1}}f(x_{i-2}) + \frac{2(\Delta_{i-2,i} + \Delta_{i+1,i})}{\Delta_{i-2,i-1}\Delta_{i-1,i}\Delta_{i-1,i+1}}f(x_{i-1}) \\ & + \frac{2(\Delta_{i-2,i} + \Delta_{i-1,i} + \Delta_{i+1,i})}{\Delta_{i-2,i}\Delta_{i-1,i}\Delta_{i+1,i}}f(x_i) + \frac{2(\Delta_{i-2,i} + \Delta_{i-1,i})}{\Delta_{i-2,i+1}\Delta_{i+1,i-1}\Delta_{i+1,i}}f(x_{i+1}) \\ & + \mathcal{O}(h^2). \end{aligned} \quad (27)$$

For the other nodes, first we consider the following four nodes $\{x_1, f(x_1)\}, \{x_2, f(x_2)\}, \{x_3, f(x_3)\}, \{x_4, f(x_4)\}$, then we similarly construct the following approximation formulas:

$$\begin{aligned} f''(x_1) = & \frac{2(\Delta_{1,2} + \Delta_{1,3} + \Delta_{1,4})}{\Delta_{1,2}\Delta_{1,3}\Delta_{1,4}}f(x_1) + \frac{2(\Delta_{3,1} + \Delta_{4,1})}{\Delta_{1,2}\Delta_{2,3}\Delta_{2,4}}f(x_2) \\ & + \frac{2(\Delta_{2,1} + \Delta_{4,1})}{\Delta_{1,3}\Delta_{3,2}\Delta_{3,4}}f(x_3) + \frac{2(\Delta_{2,1} + \Delta_{3,1})}{\Delta_{1,4}\Delta_{4,2}\Delta_{4,3}}f(x_4) \\ & + \mathcal{O}(h^2), \end{aligned} \quad (28)$$

and

$$\begin{aligned} f''(x_2) = & \frac{2(\Delta_{2,3} + \Delta_{2,4})}{\Delta_{1,2}\Delta_{1,3}\Delta_{1,4}}f(x_1) + \frac{2(\Delta_{1,2} + \Delta_{3,2} + \Delta_{4,2})}{\Delta_{1,2}\Delta_{2,3}\Delta_{2,4}}f(x_2) \\ & + \frac{2(\Delta_{1,2} + \Delta_{4,2})}{\Delta_{1,3}\Delta_{3,2}\Delta_{3,4}}f(x_3) + \frac{2(\Delta_{1,2} + \Delta_{3,2})}{\Delta_{1,4}\Delta_{4,2}\Delta_{4,3}}f(x_4) \\ & + \mathcal{O}(h^2). \end{aligned} \quad (29)$$

It is recalled that the one-sided FD formulas have larger error terms (though they are of second-order convergence).

Analogously, the adaptive FD formulas of second order for the nodes $\{x_{m-1}, x_m\}$ for approximating the second derivative of these nodes could be obtained and written in what follows:

$$\begin{aligned} f''(x_{m-1}) = & \frac{2(\Delta_{m-3,m-1} + \Delta_{m-2,m-1})}{\Delta_{m-3,m}\Delta_{m,m-2}\Delta_{m,m-1}}f(x_m) + \frac{2(\Delta_{m-3,m-1} + \Delta_{m-2,m-1} + \Delta_{m,m-1})}{\Delta_{m-3,m-1}\Delta_{m-1,m-2}\Delta_{m-1,m}}f(x_{m-1}) \\ & + \frac{2(\Delta_{m-3,m-1} + \Delta_{m,m-1})}{\Delta_{m-3,m-2}\Delta_{m-2,m-1}\Delta_{m-2,m}}f(x_{m-2}) + \frac{2(\Delta_{m-2,m-1} + \Delta_{m,m-1})}{\Delta_{m-2,m-3}\Delta_{m-1,m-3}\Delta_{m,m-3}}f(x_{m-3}) \\ & + \mathcal{O}(h^2), \end{aligned} \quad (30)$$

and

$$\begin{aligned} f''(x_m) = & \frac{2(\Delta_{m-3,m} + \Delta_{m-2,m} + \Delta_{m-1,m})}{\Delta_{m-3,m}\Delta_{m,m-2}\Delta_{m,m-1}}f(x_m) + \frac{2(\Delta_{m-3,m} + \Delta_{m-2,m})}{\Delta_{m-3,m-1}\Delta_{m-1,m-2}\Delta_{m-1,m}}f(x_{m-1}) \\ & + \frac{2(\Delta_{m-3,m} + \Delta_{m-1,m})}{\Delta_{m-3,m-2}\Delta_{m-2,m-1}\Delta_{m-2,m}}f(x_{m-2}) + \frac{2(\Delta_{m-2,m} + \Delta_{m-1,m})}{\Delta_{m-2,m-3}\Delta_{m-1,m-3}\Delta_{m,m-3}}f(x_{m-3}) \\ & + \mathcal{O}(h^2). \end{aligned} \quad (31)$$

5. The semi-discrete system

Taking into consideration the new adaptive FD formulas obtained for the diffusion and convection parts of (5), here a spatial discretization of the PDE model is given to achieve a set of linear ODEs.

To express this semi-discretization as elegantly as possible, while to keep the requirement as minimum as possible, we may gather all the discretization formulas (20)–(31) in matrix notations. This is possible since the FD approximation, is a linear operation. Accordingly, another approach for describing the impact of (20)–(31) is with matrices consisting of the coefficients of (20)–(31), i.e., the adaptive FD weights, as their elements.

Summarizing all the adaptive weights coming from convection, diffusion and reaction terms altogether, a coefficient matrix $B(t)$ can be deduced in the following form:

$$\begin{aligned} B(t) = & \frac{1}{2} \mathbf{S}^2 \mathbf{V} (D_{ss} \otimes I_v \otimes I_r) + \frac{1}{2} \sigma_1^2 \mathbf{V} (I_s \otimes D_{vv} \otimes I_r) \\ & + \frac{1}{2} \sigma_2^2 (I_s \otimes I_v \otimes D_{rr}) + \rho_{12} \sigma_1 \mathbf{S} \mathbf{V} (D_s \otimes D_v \otimes I_r) \\ & + \rho_{13} \sigma_2 \mathbf{S} (\mathbf{V})^{\frac{1}{2}} (D_s \otimes I_v \otimes D_r) + \rho_{23} \sigma_1 \sigma_2 (\mathbf{V})^{\frac{1}{2}} (I_s \otimes D_v \otimes D_r) \\ & + \mathbf{R} \mathbf{S} (D_s \otimes I_v \otimes I_r) + \kappa (\eta I - \mathbf{V}) (I_s \otimes D_v \otimes I_r) \\ & + a(b(T-t)I - \mathbf{R})(I_s \otimes I_v \otimes D_r) - rI, \end{aligned} \quad (32)$$

wherein

$$I = I_s \otimes I_v \otimes I_r, \quad (33)$$

is a unit matrix of the dimension $N \times N$, $N = m \times n \times o$, I_s is the unit matrix of the dimension $m \times m$ along s , and similarly for I_v and I_r . The square matrices D_s , D_v , D_r , D_{ss} , D_{vv} , and D_{rr} , are constructed based on the adaptive weights in Section 4. Moreover, the diagonal matrices \mathbf{S} , \mathbf{V} and \mathbf{R} are given by:

$$\mathbf{S} = \text{diag}(s_1, s_2, \dots, s_m) \otimes I_v \otimes I_r, \quad (34)$$

$$\mathbf{V} = I_s \otimes \text{diag}(v_1, v_2, \dots, v_n) \otimes I_r, \quad (35)$$

$$\mathbf{R} = I_s \otimes I_v \otimes \text{diag}(r_1, r_2, \dots, r_o). \quad (36)$$

Therefore, the PDE model can be semi-discretized and a set of time-continuous linear ODEs could be constructed as follows:

$$U'(t) = B(t)U(t), \quad 0 \leq t \leq T, \quad (37)$$

where

$$U(0) = \phi(s, v, r), \quad (38)$$

and $U(t) = (u_{1,1,1}(t), u_{1,1,2}(t), \dots, u_{m,n,o-1}(t), u_{m,n,o}(t))^*$, is the vector of unknowns. The $N \times 1$ vector function of time $U(t)$ is called the state vector, and its components are the state variables.

The coefficient matrix $B(t)$ is not constant in general since the deterministic function b in (5) is time-dependent. Additionally, the matrix $B_{N \times N}(t)$ due to the semi-discretization of the PDE problem (5) has been obtained without imposing the boundaries until now.

6. Incorporating the boundary conditions

Boundary conditions describe the financial characteristics of the contract at boundary values of the underlying price process [24]. The boundary conditions given for (5) are of mixed type. Since the model is a 3D PDE, so (at least) conditions for six faces of the computational domain should be given.

The conditions on the boundary for the s -direction are given by:

$$u(s, v, r, t) = 0, \quad s = 0, \quad (39)$$

$$\frac{\partial u}{\partial s}(s, v, r, t) = 1, \quad s = s_{\max}. \quad (40)$$

At the boundary $v = v_{\max}$, the following Dirichlet condition is prescribed:

$$u(s, v, r, t) = s, \quad v = v_{\max}. \quad (41)$$

These boundary conditions are quite familiar due to Heston stochastic volatility problem [4]. At the boundary $v = 0$, the PDE is degenerate, and accordingly no special boundary is incorporated at this face. Following a discussion given in [25], it is assumed that the discretized equations for nodes located on this boundary are the artificial boundaries.

Finally, when $r = \pm r_{\max}$, the following Neumann boundary conditions are prescribed:

$$\frac{\partial u}{\partial r}(s, v, r, t) = 0, \quad r = r_{\max}, \quad (42)$$

$$\frac{\partial u}{\partial r}(s, v, r, t) = 0, \quad r = -r_{\max}. \quad (43)$$

In this work, we impose all the boundary conditions by differentiating the boundary conditions against the time variable and then resolving for the obtained differential equation(s), viz, imposing the new equations into the system of ODEs at the equations which correspond to the same node on the boundary using a similar methodology as in [26].

At the end, after imposing the boundaries, we attain the following system of semi-discretized (linear) ODEs subject to a non-smooth payoff function (7):

$$U'(t) = \bar{B}(t)U(t) = G(t, U(t)), \quad (44)$$

where $\bar{B}(t)$ is the coefficient matrix which includes the boundaries. This matrix consists of several zero rows due to incorporating the Dirichlet boundary conditions at two faces of the computational domain.

The coefficient matrix $\bar{B}(t)$ in (44) is time dependent and continuous on an interval in \mathbb{R} . The continuous, real-valued matrix function $\bar{B}(t)$ in the time-varying system (44) is singular due to imposing the boundary conditions into this coefficient matrix directly.

The initial value problem (44) satisfies the conditions of the existence and uniqueness theorem [27], we have

$$\|\bar{B}(t)U_1(t) - \bar{B}(t)U_2(t)\| \leq \mathcal{L}\|U_1(t) - U_2(t)\|, \quad (45)$$

for some $\mathcal{L} > 0$.

We can state that if the matrix-function $\bar{B}(t)$ be continuous on some interval $I \subseteq \mathbb{R}$, then the solution to (44) exists, unique and extends to the whole working interval.

7. Stability and full discretization

For linear homogeneous set of ODEs (44), the solution is a continuously-differentiable, $n \times 1$ function $U(t)$ that satisfies (44) for all t , though at the outset only solutions for $0 \leq t \leq T$ are considered.

The exact solution of the linear state system (44) can be written in what follows:

$$U(t) = \Theta(t, t_0)U(t_0), \quad (46)$$

at which the transition matrix $\Theta(t, t_0)$ is defined by

$$\begin{aligned} \Theta(t, t_0) = & I + \int_{t_0}^t \bar{B}(\sigma_1) d\sigma_1 \\ & + \int_{t_0}^t \bar{B}(\sigma_1) \int_{t_0}^{\sigma_1} \bar{B}(\sigma_2) d\sigma_2 d\sigma_1 \\ & + \int_{t_0}^t \bar{B}(\sigma_1) \int_{t_0}^{\sigma_1} \bar{B}(\sigma_2) \int_{t_0}^{\sigma_2} \bar{B}(\sigma_3) d\sigma_3 d\sigma_2 d\sigma_1 + \dots, \end{aligned} \quad (47)$$

wherein I is the unit matrix of an appropriate size. It is convenient to view the transition matrix $\Theta(t, t_0)$ in (46) as a function of two variables, defined by the Peano–Baker series (47). In our system (44) $t_0 = 0$. The series (47) converges uniformly and absolutely for any $t \in [-T, T]$, see [28, page 46] for a complete theoretical discussion.

The Peano–Baker series is a basic theoretical tool for ascertaining properties of solutions of linear state equations. The analytic solution based on (47) requires the computation of infinite number of integrals of matrix functions, which are *tremendously time-consuming*. To avoid these, one may rely on temporal discretization via numerical time-stepping methods [29].

In terms of having a unique solution for (44), a proof can be accomplished by showing that any two solutions necessarily are identical.

It is natural to begin by characterizing stability of the linear state equation (44) in terms of bounds on the transition matrix $\Theta(t, t_0)$ for $\bar{B}(t)$. This leads to a well-known eigenvalue condition when $\bar{B}(t)$ is constant, but does not provide a generally useful stability test for time-varying cases because of the difficulty of computing $\Theta(t, t_0)$, [28, chapter 6]. In fact, it might be thought that the pointwise-in-time eigenvalues of $\bar{B}(t)$ could be used to characterize internal stability properties of a linear state equation (44). But this is not true in general.

Authors in [30] discussed that even the implicit Euler's method which is unconditionally stable for linear systems when all the eigenvalues of the coefficient matrix have negative real parts, is not stable and a sufficiently small step size is required for the time-varying cases.

The system (44) is called uniformly exponentially stable if there exist finite positive constants δ and ϵ such that for any t_0 , the corresponding solution satisfies

$$\|U(t)\| \leq \delta \exp(-\epsilon(t - t_0))\|U(0)\|, \quad t \geq t_0, \quad (48)$$

wherein δ is independent of t_0 .

The property of uniform exponential stability can be expressed in terms of an exponential bound on the transition matrix. Furthermore using (48), it is obvious to deduce that

$$\|\Theta(t, t_0)\| \leq \delta \exp(-\epsilon(t - t_0)), \quad t \geq t_0. \quad (49)$$

To connect the notions of stability and convergence for such time-varying systems, let us take into account that its solution is such that $\|U(t)\|^2$ monotonically decreases as $t \rightarrow \infty$. The derivative of the scalar function

$$\|U(t)\|^2 = U^*(t)U(t), \quad (50)$$

with respect to t can now be written as

$$\begin{aligned} \frac{d}{dt} \|U(t)\|^2 &= \dot{U}^*(t)U(t) + U^*(t)\dot{U}(t) \\ &= U^*(t)[\bar{B}^*(t) + \bar{B}(t)]U(t). \end{aligned} \quad (51)$$

Noting that throughout this section, $*$ stands for the transpose notation. Now $\dot{U}(t)$ is replaced by $\bar{B}(t)U(t)$ precisely because $U(t)$ is a solution of (44). Suppose that the quadratic form on the right side of (51) is negative definite, that is, suppose the matrix $\bar{B}^*(t) + \bar{B}(t)$ is negative definite at each t . Then $\|U(t)\|^2$ decreases as t increases. Further, it can be observed that if this negative definiteness does not asymptotically vanish, that is, if there is a constant $\alpha > 0$ such that

$$\bar{B}^*(t) + \bar{B}(t) \leq -\alpha I, \quad (52)$$

for all t , then $\|U(t)\|^2$ goes to zero as $t \rightarrow \infty$.

Theorem 7.1 ([28, page 132]). *For the linear state equation (44), denote the largest and smallest pointwise eigenvalues of $\bar{B}^*(t) + \bar{B}(t)$ by $\lambda_{\max}(t)$ and $\lambda_{\min}(t)$. Then, the solution of (44) satisfies*

$$\|U(0)\| \exp\left(\frac{1}{2} \int_{t_0}^t \lambda_{\min}(\sigma) d\sigma\right) \leq \|U(t)\| \leq \|U(0)\| \exp\left(\frac{1}{2} \int_{t_0}^t \lambda_{\max}(\sigma) d\sigma\right), \quad (53)$$

for all $t \geq t_0$.

Theorem 7.1 leads to easy proofs of some simple stability criteria based on the eigenvalues of $\bar{B}^*(t) + \bar{B}(t)$. As a matter of fact, for the linear state equation (44), denote the largest and smallest pointwise eigenvalues of $\bar{B}^*(t) + \bar{B}(t)$ by $\lambda_{\max}(t)$ and $\lambda_{\min}(t)$. Then it is uniformly stable if there exists a finite constant δ such that the largest pointwise eigenvalue of $\bar{B}^*(t) + \bar{B}(t)$ satisfies

$$\int_{t_0}^t \lambda_{\max}(\sigma) d\sigma \leq \delta, \quad (54)$$

for all t, t_0 , such that $t \geq t_0$. Furthermore, it is uniformly exponentially stable if there exist finite, positive constants δ and ϵ , such that

$$\int_{t_0}^t \lambda_{\max}(\sigma) d\sigma \leq -\epsilon(t - t_0) + \delta. \quad (55)$$

Now assume that the coefficient matrix $\bar{B}(t)$ in (44) is bounded. Furthermore, let us denote \mathbf{u}_t as an approximate solution to the exact value $\mathbf{u}(t_i)$. By choosing $\varpi + 1$ temporal nodes and a temporal step size

$$\Delta t = \frac{T}{\varpi} > 0, \quad (56)$$

we have

$$t_{i+1} = t_i + \Delta t, \quad 0 \leq i \leq \varpi, \quad (57)$$

and $\mathbf{u}_0 = \mathbf{u}(s, v, r, 0)$. Then, the explicit forward Euler's method [26, page 16] could be written as follows:

$$\mathbf{u}_{i+1} = \mathbf{u}_i + \Delta t G(t_i, \mathbf{u}_i) + \mathcal{O}(\Delta t^2). \quad (58)$$

Note that along with (55) one may use error estimates for stability control for (58), since there does not seem to be a straightforward way of controlling the stability of an asymptotically contracting, non-autonomous, linear, scalar test problem without some type of error control, see for more [31].

However, by considering the explicit Euler's method with the local truncation error of order $p = 2$, there exists Δt , for which the numerical solution (58) is discretely asymptotically contracting [31].

Theorem 7.2. *Assume that the function G satisfies Lipschitz condition with Lipschitz constant \mathcal{L} and (54) holds. Then, the constructed proposed scheme for pricing (5) when $h \rightarrow 0$, (as the maximum local spacings) via the semi-discretized system of ODEs (44) & (58) is conditionally time-stable, i.e., for all sufficiently small Δt , say,*

$$\Delta t < \frac{1}{\mathcal{L}}, \quad (59)$$

the scheme (58) is stable in L^2 norm.

Proof. Let $T = \varpi \Delta t$, and

$$e_{i+1} = \hat{u}_{i+1} - u_{i+1}, \quad (60)$$

where $\hat{u}_{\iota+1}$ and $u_{\iota+1}$ are exact and approximation solutions of Eq. (58), respectively. Accordingly, we have

$$e_{\iota+1} = e_\iota + \Delta t (G(t, \hat{u}_\iota) - G(t, u_\iota)), \quad (61)$$

Multiplying (61) by $e_{\iota+1}$ and integrating on $[0, T]$, one has

$$\langle e_{\iota+1}, e_{\iota+1} \rangle = \langle e_\iota, e_{\iota+1} \rangle + \Delta t \langle G(t, \hat{u}_\iota) - G(t, u_\iota), e_{\iota+1} \rangle, \quad (62)$$

where $\langle \cdot, \cdot \rangle$ denotes the standard L^2 inner product. By the Schwarz inequality [32, p. 1099] and Lipschitz condition, we can write

$$\|e_{\iota+1}\|_2^2 \leq \frac{1}{2} (\|e_\iota\|_2^2 + \|e_{\iota+1}\|_2^2) + \mathcal{L} \Delta t \frac{1}{2} (\|e_\iota\|_2^2 + \|e_{\iota+1}\|_2^2) \quad (63)$$

Rearranging (63), we have

$$2\|e_{\iota+1}\|_2^2 \leq (1 + \mathcal{L} \Delta t) \|e_\iota\|_2^2 + (1 + \mathcal{L} \Delta t) \|e_{\iota+1}\|_2^2, \quad (64)$$

and using (59), we obtain

$$\|e_{\iota+1}\|_2^2 \leq \frac{1 + \mathcal{L} \Delta t}{1 - \mathcal{L} \Delta t} \|e_\iota\|_2^2. \quad (65)$$

Subsequently, one can find for $\iota = 0, 1, \dots, \varpi$, that

$$\|e_{\iota+1}\|_2^2 \leq \left(\frac{1 + \mathcal{L} \Delta t}{1 - \mathcal{L} \Delta t} \right)^\iota \|e_0\|_2^2. \quad (66)$$

Now, when $\iota \rightarrow \varpi$ and $\varpi \rightarrow \infty$, we obtain

$$\lim_{\iota \rightarrow \infty} \left(\frac{1 + \mathcal{L} \Delta t}{1 - \mathcal{L} \Delta t} \right)^\iota = \exp(2\mathcal{L}T) < \infty, \quad (67)$$

since $\Delta t = T/\varpi$. The relations (66) and (67), show that

$$\lim_{\iota \rightarrow \infty} \|e_{\iota+1}\|_2^2 = 0. \quad (68)$$

Thus, the propagation of the error can be controlled via (59). This ends the proof. \square

The motivation of choosing (58) is for its simplicity in coding. Per computing step, it requires the calculation of one functional evaluations, that is, one $\bar{B}(t)$ and this helps the program to be run faster than some of its competitors such as Exponential Time Differencing (ETD) scheme [33], which require several calculation of the action of matrix exponential on a vector per step size, as well as the Runge–Kutta methods that demand more computations of the $\bar{B}(t)$ per cycle to proceed. This increases the computational efficiency of the proposed approach (44) & (58) for tackling (5).

In practical computations, it is necessary to know much about \mathcal{L} . In fact, the inequality (45) reveals that, one may choose \mathcal{L} as follows:

$$\mathcal{L} = \max_{0 \leq t \leq T} \sigma_{\max}(\bar{B}(t)), \quad (69)$$

where $\sigma_{\max}(\cdot)$ is the largest singular value of the matrix $\bar{B}(t)$. This value even for very scale matrices can quickly be calculated via the command `SingularValueList[matrix, 1]` in Mathematica 11.0 or in other modern programming languages.

Another observation here is that the bound in (59) is tight meaning that even a bit looser choice for the temporal step size could yield the solution in a stable form. So, we can also write the following inequality loosening (59) as follows:

$$0 < \Delta t < \frac{1}{\mathcal{L}} < \frac{-2}{\text{Re}(\chi)}, \quad (70)$$

wherein

$$\chi = \max_{0 \leq t \leq T} \lambda_{\max}(\bar{B}(t)). \quad (71)$$

Once needed for the computation of the new bound (71) based on the largest eigenvalue $\lambda_{\max}(\cdot)$, one can do such a thing based on the command `Eigenvalues[matrix, 1]`.

8. Computational results

Here, extensive financial experiments are discussed for solving (5) in case of at-the-money options. This results in significant insight in their real stability and convergence speed in the presence of truncation and round-off errors. A comparison is given with the standard FD method [34, chapters 9–10], which is based on second order FD approximations and Euler's method for time-stepping denoted by FD, the nonuniform method (based on Douglas time-stepping solver with $\theta = 0$) given in [19] denoted by HM, while the proposed FDM (44) & (58) is denoted by AFD.

Table 1
Parameter settings for the HHW PDE.

	T	E	κ	η	a	σ_1	σ_2	ρ_{12}	ρ_{13}	ρ_{23}	c_1	c_2	c_3
Case I	1	100	3.0	0.12	0.20	0.80	0.03	0.6	0.2	0.4	0.05	0	0
Case II	1	100	0.5	0.8	0.16	0.90	0.03	-0.5	0.2	0.1	0.055	0	0
Case III	0.25	100	1.0	0.09	0.22	1.00	0.07	-0.3	-0.5	-0.2	0.074	0.014	2.10

The simulations are run on an office laptop with Windows 7 Ultimate equipped with Intel(R) Core(TM) i5-2430M CPU 2.40 GHz processor and 16.00 GB of RAM on a 64-bit operating system. Additionally, the computer programs are written in Mathematica 11.0 by setting AccuracyGoal → 5, PrecisionGoal → 5, [35, chapter 1.11]. The time needed to obtain the option prices will be denoted by *time* in seconds. The following relative error measure is used for comparisons:

$$RE = \left| \frac{u_{\text{approx}}(s, v, r, t) - u_{\text{ref}}(s, v, r, t)}{u_{\text{ref}}(s, v, r, t)} \right|, \quad (72)$$

where u_{ref} and u_{approx} are the reference and approximate solutions. The reference solutions are extracted based on very refined grids along all the variables, s , v and r as well as with a very small temporal step size.

Experimental results revealed that the higher number of nodes along s , the higher accuracy in the final computed price. Hence, here we mainly select more number nodes along s rather than the other spatial variables, v and r . Here, some inquiries may be arisen such as: Why is this? Does this mean that the solution accuracy is sensitive to the finest of s and not on v and/or r ? Is it due to the proposed nonuniform scheme or is it because of the nature of the HHW model? To answer, first the nature of the HHW PDE-based model made us to focus on special parts of the computational domain. Second, the discretization interval for s is so large and because of this it almost requires two times more number of points. Besides, the non-differentiability of the initial condition affect along this spatial variable. And third this consideration is not related to the structure of the proposed FD scheme.

Different comparison cases are given in Table 1, when the deterministic function b is constant and non-constant. The non-constant b is defined as follows:

$$b(\tau) = c_1 - c_2 \exp(-c_3 \tau), \quad \tau \geq 0, \quad (73)$$

where c_1, c_2, c_3 are constant, and $\tau = T - t$.

Table 2 shows a comparison among the existing methods and the proposed scheme for Case I considering the reference solution $u(100, 0.04, 0.1, 1) \simeq 16.10$. It reveals that AFD is better than the FD and the HM methods. From numerical results we observe that accuracy in successive approximations increases, showing stable nature of the methods. Also, the presented method shows consistent convergence behavior. Figs. 2–3 are furnished based on AFD with $m = 45$, $n = 22$, $o = 22$ and $\Delta t = 0.000025$.

Although based on Table 2, FD converges to the solution slowly, it does not preserve the positivity of the solution. In fact, because of applying uniform grids, there is an instability in the computed solution as illustrated in Fig. 4.

The results for Case II are shown in Table 3, using different number of discretization points. Similarly the reference value is considered at the hot zone $u(100, 0.04, 0.1, 1) \simeq 20.97$.

It can be observed from the numerical results of Tables 2–3 that like the existing methods the proposed adaptive FDM is well-behaved. It is clear that the accuracy in numerical values of approximations to the reference prices by AFD is higher than the existing algorithms in general.

Case III is important since it leads to a time varying large sparse banded matrix $\bar{B}(t)$, which is harder to deal with via time-stepping solvers. The choice of the function b is to some extent arbitrary, but the conclusions we attain here are valid also for other choices. The results show a stable and positive computational solution.

Fig. 5 shows the numerical solution based on AFD in Case III. It reveals a smooth numerical solution without any oscillations for the proposed scheme while keeping the positivity of the solution. Fig. 6 illustrates that our scheme is convergent by increasing the size at the hot zone $(100, 0.04, 0.1, 1)$, when $m = 24$, $n = 14$, $o = 14$, $\Delta t = 0.00005$. Noting that solving the system of ODEs in this case with a varying coefficient matrix is time-consuming.

Finally, to clearly reveal the stability discussion given in Section 7 for the time-varying linear system, the same settings as in Case III is taken into account using AFD and $m = 14$, $n = o = 8$ and $\Delta t = 0.0005$. In this case, the eigenvalues of the coefficient matrix $\bar{B}(t)$ are plotted in Fig. 7, which shows that in such time-varying linear systems even in the presence of eigenvalues with positive real parts, an enough small step size for the Euler's method would result in a stable method.

An important issue here is that the choice (73) and its parameters c_2 and c_3 play a crucial role in having eigenvalues with negative real parts. Clearly, large values for c_2 and c_3 may result in eigenvalues with large positive real parts, which require a very small Δt . However, for a slowly-varying linear system (44), the important condition (54) along with the bound (59) can present a conditional stability for the proposed approach.

As can be observed in this section, for different types of the European call options, the proposed approach illustrated a fast and reliable approach which needs fewer number of computational nodes for converging, while it keeps positivity and stability of the numerical solution in contrast to the existing solvers in the literature.

Table 2
Results of comparisons for Case I.

Method	m	n	σ	Size	Δt	Price	RE	Time
FD								
	10	8	6	480	0.002	25.4927	5.8320×10^{-1}	0.39
	14	10	10	1400	0.001	11.0989	3.1071×10^{-1}	0.62
	18	12	12	2592	0.0005	17.2031	6.8388×10^{-2}	1.22
	24	14	14	4704	0.00025	18.7318	1.6332×10^{-1}	3.39
	28	16	16	7168	0.0002	13.3292	1.7219×10^{-1}	6.07
	45	22	22	21780	0.00005	14.6364	9.1017×10^{-2}	70.54
	50	24	22	26400	0.00004	16.1685	4.1337×10^{-3}	103.32
HM								
	10	8	6	480	0.001	14.4724	1.0120×10^{-1}	0.44
	14	10	10	1400	0.0005	15.3002	4.9790×10^{-2}	0.85
	18	12	12	2592	0.00025	15.6158	3.0191×10^{-2}	2.09
	24	14	14	4704	0.0001	15.8066	1.8340×10^{-2}	8.04
	28	16	16	7168	0.0001	15.8712	1.4331×10^{-2}	11.84
	45	22	22	21780	0.000025	15.9948	6.6574×10^{-3}	130.04
AFD								
	10	8	6	480	0.001	17.8051	1.0577×10^{-1}	0.50
	14	10	10	1400	0.0005	17.6668	9.7183×10^{-2}	0.91
	18	12	12	2592	0.00025	16.6932	3.6717×10^{-2}	2.12
	24	14	14	4704	0.0001	16.3073	1.2750×10^{-2}	9.22
	28	16	16	7168	0.0001	16.2224	7.4809×10^{-3}	12.24
	45	22	22	21780	0.000025	16.1140	7.4624×10^{-4}	152.66

Table 3
Results of comparisons for Case II.

Method	m	n	σ	Size	Δt	Price	RE	Time
FD								
	20	10	10	2000	0.00025	22.0223	4.9885×10^{-2}	1.77
	24	12	12	3456	0.0002	21.4365	2.1957×10^{-2}	3.14
	26	14	14	5096	0.0001	19.6784	6.1859×10^{-2}	8.67
	28	16	16	7168	0.0001	17.3762	1.7161×10^{-1}	11.72
	30	18	18	9720	0.00005	17.4042	1.7028×10^{-1}	35.50
	36	20	20	14400	0.000025	20.5104	2.2196×10^{-2}	107.89
	38	22	22	18392	0.000025	20.2757	3.3383×10^{-2}	161.16
	42	22	22	20328	0.00002	18.3706	1.2420×10^{-1}	244.32
HM								
	20	10	10	2000	0.00025	20.6314	1.6426×10^{-2}	1.69
	24	12	12	3456	0.0002	20.7096	1.2696×10^{-2}	3.40
	26	14	14	5096	0.0001	20.7290	1.1771×10^{-2}	8.64
	28	16	16	7168	0.0001	20.7482	1.0858×10^{-2}	12.36
	30	18	18	9720	0.00005	20.7673	9.9464×10^{-3}	36.54
	36	20	20	14400	0.000025	20.8109	7.8705×10^{-3}	108.92
	38	22	22	18392	0.000025	20.8182	7.5196×10^{-3}	166.08
	42	22	22	20328	0.00002	20.8333	6.7988×10^{-3}	250.67
AFD								
	20	10	10	2000	0.00025	21.3221	1.6502×10^{-2}	1.79
	24	12	12	3456	0.0002	21.1079	6.2892×10^{-3}	3.50
	26	14	14	5096	0.0001	21.0847	5.1844×10^{-3}	9.51
	28	16	16	7168	0.0001	21.0693	4.4487×10^{-3}	13.29
	30	18	18	9720	0.00005	21.0489	3.4780×10^{-3}	38.50
	36	20	20	14400	0.000025	21.0078	1.5197×10^{-3}	109.12
	38	22	22	18392	0.000025	20.9989	1.0937×10^{-3}	169.81
	42	22	22	20328	0.00002	20.9833	3.5113×10^{-4}	262.54

9. Final remarks

A pivotal feature of options is to furnish a tool in order to control the market risk. Computational schemes which are quite reliable and fast are one of the only choices for tackling option pricing (in the multi-dimensional cases) because of the complexity of the underlying processes. One of the important financial models at which all the asset price, its variance and

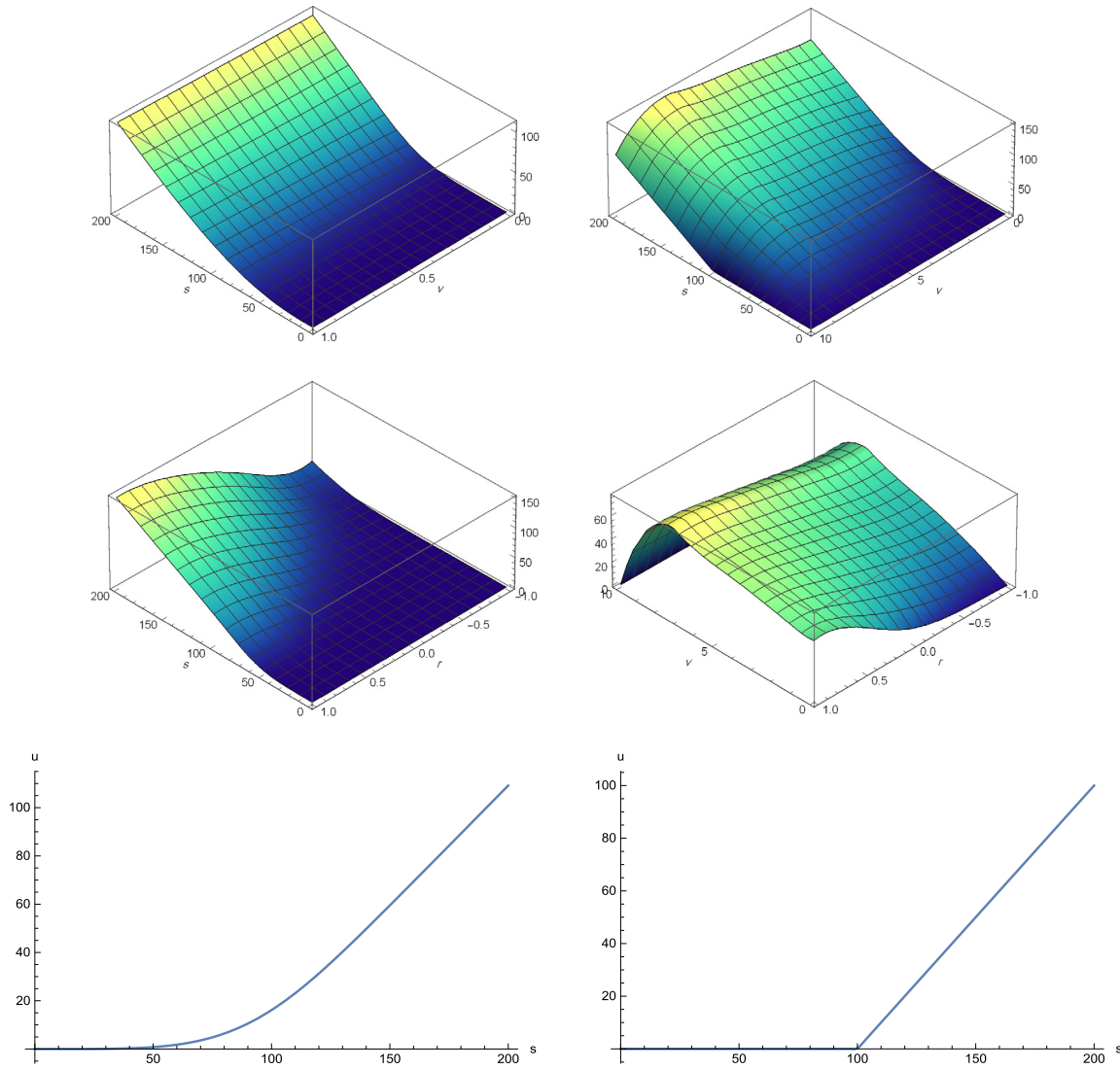


Fig. 2. The computational solution based on AFD in Case I for $u(s, v, 0.1, 1)$ (top-left), for $u(s, v, 0.1, 1)$ but for the whole domain of v (top-right). $u(s, 0.04, r, 1)$ (middle-left) and $u(100, v, r, 1)$ (middle-right). The solution when $u(s, 0.04, 0.1, 1)$ (bottom-left) and the solution when $u(s, 10, 1, 1)$ (bottom-right).

its interest rate are coming from stochastic processes, while the interest rate could also take negative values were introduced and studied under the HHW PDE-based model.

Toward this objective, new higher order adaptive FD discretizations were obtained on non-uniform grids, at which the concentration is much more focused on the hotzone. In the proposed spatial discretization, approximation formulas are of third-order accuracy for the convection terms, while they are of second-order accuracy for the diffusion parts. Under these FD formulas, the semi-discretized set of equations for the HHW PDE was obtained and it was shown that it satisfies the existence and uniqueness of having a solution. The system of ODEs with a varying coefficient matrix was tackled using a time-stepping method. It was discussed that under several conditions the new computational scheme is stable.

Several tests from finance were also worked out in detail. All computations are performed in the programming package Mathematica using double-precision arithmetic. In the comparison of performance of the methods, we have included the CPU-times utilized in the execution of the written programs. The acceleration of convergence speed was attained without any special (or high burden) on the sparsity pattern of the coefficient matrix, thus, the contributed FDM possesses a higher computational efficiency.

Some discussion and further improvements would stay for future studies including the application of spectral methods, which results in dense matrices but with exponential convergence rate, as well as the parallelization of the proposed approach on GPUs.

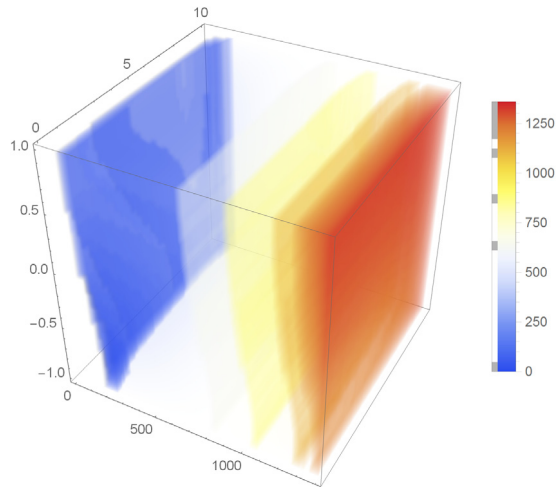


Fig. 3. The density plot of the solution in Case I applying AFD, revealing that the solution keeps the positivity.

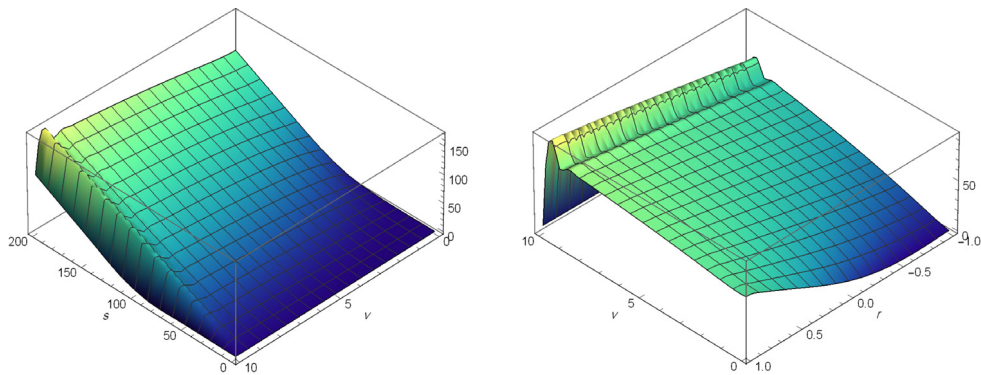


Fig. 4. Unstable solution based on FD in Case I for $u(s, v, 0.1, 1)$ (left) and $u(100, v, r, 1)$ (right).

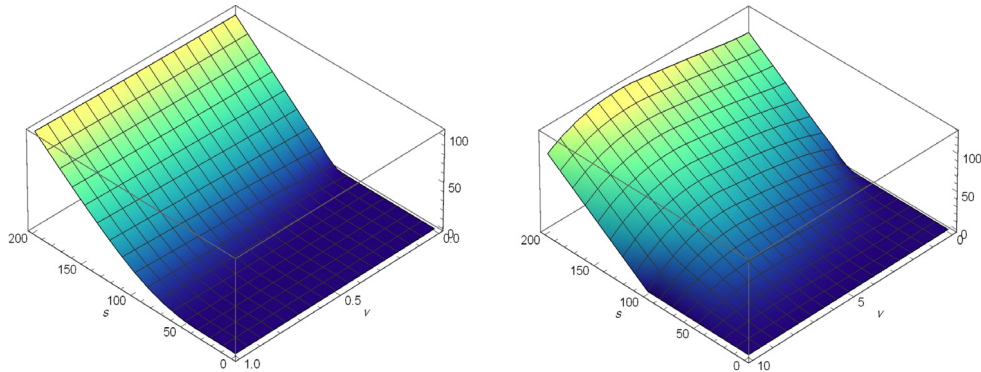


Fig. 5. Numerical solution based on AFD in Case III for $u(s, v, 0.1, 1)$ (left) and $u(s, v, 0.1, 1)$ (right) in different domains.

Apart from these, investigation on recent and new methods of the literature such as the hp-proper orthogonal decomposition moving least squares approach discussed deeply in [36] and the two-field reduced basis approximation introduced in [37], (which includes adaptive selection of sampling parameter points) could be focused for forthcoming works.

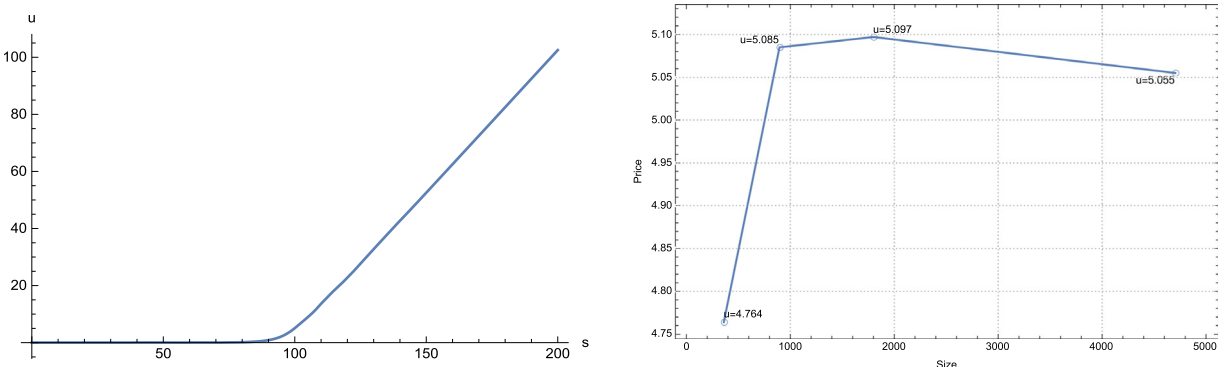


Fig. 6. Numerical solution based on AFD in Case III for $u(s, 0.04, 0.1, 1)$ (left) and its convergence history (right).

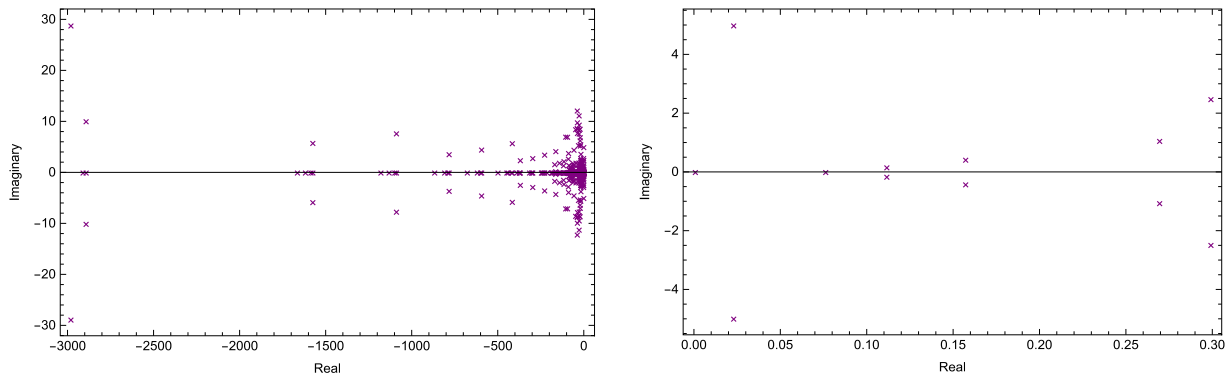


Fig. 7. The eigenvalues of $\bar{B}(0)$ using AFD in Case III, all the eigenvalues in (left), while the eigenvalues with positive real parts are drawn in (right).

Acknowledgments

The authors are grateful to three anonymous referees for many comments, which helped the readability and reliability of the present article.

References

- [1] W.T. Shaw, Modelling Financial Derivatives with Mathematica, Cambridge University Press, UK, 1998.
- [2] M. Briani, L. Caramellino, A. Zanette, A hybrid tree/finite-difference approach for Heston-Hull-White type models, *J. Comput. Finance* 21 (2017) 1–45.
- [3] J. Hull, A. White, The general Hull–White model and supercalibration, *Financ. Anal. J.* 57 (2001) 34–43.
- [4] S.L. Heston, A closed-form solution for options with stochastic volatility with applications to bond and currency options, *Rev. Financ. Stud.* 6 (1993) 327–343.
- [5] R. Schöbel, J. Zhu, Stochastic volatility with an Ornstein–Uhlenbeck process: an extension, *Eur. Financ. Rev.* 3 (1999) 23–46.
- [6] A. Van Haastrecht, R. Lord, A. Pelsser, D. Schrager, Pricing long-maturity equity and FX derivatives with stochastic interest rates and stochastic volatility, *Insurance Math. Econ.* 45 (2009) 436–448.
- [7] J.C. Cox, J.E. Ingersoll, S.A. Ross, A theory of the term structure of interest rates, *Econometrica* 53 (1985) 385–407.
- [8] J. Cao, G. Lian, T.R.N. Roslan, Pricing variance swaps under stochastic volatility and stochastic interest rate, *Appl. Math. Comput.* 277 (2016) 72–81.
- [9] H.Y. Wong, J. Zhao, An artificial boundary method for the Hull–White model of American interest rate derivatives, *Appl. Math. Comput.* 217 (2011) 4627–4643.
- [10] J. Hull, A. White, Using Hull–White interest rate trees, *J. Derivatives* 4 (1996) 26–36.
- [11] L.A. Grzelak, C.W. Oosterlee, S. Van Weeren, Extension of stochastic volatility equity models with the Hull–White interest rate process, *Quant. Finance* 12 (2009) 89–105.
- [12] D. Brigo, F. Mercurio, Interest Rate Models—Theory and Practice: With Smile, Inflation and Credit, second ed., Springer Finance, Springer-Verlag, Berlin, 2007.
- [13] L.A. Grzelak, C.W. Oosterlee, On the Heston model with stochastic interest rates, *SIAM J. Financ. Math.* 2 (2011) 255–286.
- [14] F. Black, P. Karasinski, Bond and option pricing when short rates are lognormal, *Financ. Anal. J.* 47 (1991) 52–59.
- [15] G. Fusai, A. Roncoroni, Implementing Models in Quantitative Finance: Methods and Cases, Springer-Verlag, Berlin, 2008.
- [16] O. Samimi, Z. Mardani, S. Sharafpour, F. Mehrdoust, LSM algorithm for pricing American option under Heston–Hull–White's stochastic volatility model, *Comput. Econ.* 50 (2017) 173–187.
- [17] V.V. Piterbarg, Smiling hybrids, *Risk Mag. Ltd.* 19 (2006) 66–71.
- [18] L.A. Grzelak, C.W. Oosterlee, On cross-currency models with stochastic volatility and correlated interest rates, *Appl. Math. Finance* 19 (2012) 1–35.

- [19] T. Haentjens, K.J. In't Hout, Alternating direction implicit finite difference schemes for the Heston–Hull–White partial differential equation, *J. Comput. Finance* 16 (2012) 83–110.
- [20] R. Knapp, A method of lines framework in Mathematica, *J. Numer. Anal. Ind. Appl. Math.* 3 (2008) 43–59.
- [21] N. Thakoor, D.Y. Tangman, M. Bhuruth, RBF-FD schemes for option valuation under models with price-dependent and stochastic volatility, *Eng. Anal. Bound. Elem.* 92 (2018) 207–217.
- [22] K. Atkinson, W. Han, *Theoretical Numerical Analysis. A Functional Analysis Framework*, third ed., Springer, New York, 2009.
- [23] B. Fornberg, *A Practical Guide to Pseudospectral Methods*, Cambridge University Press, UK, 1996.
- [24] J. Hozman, T. Tichý, On the impact of various formulations of the boundary condition within numerical option valuation by DG method, *Filomat* 30 (2016) 4253–4263.
- [25] E. Ekström, J. Tysk, Boundary conditions for the single-factor term structure equation, *Ann. Appl. Probab.* 21 (2011) 332–350.
- [26] M. Sofroniou, R. Knapp, *Advanced Numerical Differential Equation Solving in Mathematica*, Wolfram Mathematica, Tutorial Collection, USA, 2008.
- [27] A.S. Novozhilov, Lecture Notes: Ordinary Differential Equations I, Non-Autonomous Linear Systems of ODE, General Theory, USA, pp. 74–86.
- [28] W.J. Rugh, *Linear System Theory*, second ed. New Jersey, 1996.
- [29] R.K. Miller, A.N. Michel, *Ordinary Differential Equations*, Dover Publications, USA, 2007.
- [30] A.J. Steyer, E.S. Van Vleck, A Lyapunov and Sacker-Sell spectral stability theory for one-step methods, *BIT* 58 (2018) 749–781.
- [31] A.J. Steyer, A Lyapunov exponent based stability theory for ordinary (Ph.D. Thesis), USA, 2016.
- [32] I.S. Gradshteyn, I.M. Ryzhik, *Tables of Integrals, Series, and Products*, sixth ed., Academic Press, San Diego, CA, 2000.
- [33] J. Loffeld, M. Tokman, Comparative performance of exponential, implicit, and explicit integrators for stiff systems of ODEs, *J. Comput. Appl. Math.* 241 (2013) 45–67.
- [34] D.J. Duffy, *Finite Difference Methods in Financial Engineering: A Partial Differential Equation Approach*, Wiley, England, 2006.
- [35] M. Trott, *The Mathematica Guidebook for Numerics*, Springer, New York, NY, USA, 2006.
- [36] K.C. Hoang, Y.Y. Fu, J.H. Song, An hp-proper orthogonal decomposition-moving least squares approach for molecular dynamics simulation, *Comput. Methods Appl. Mech. Engrg.* 298 (2016) 548–575.
- [37] K.C. Hoang, T.Y. Kim, J.H. Song, Fast and accurate two-field reduced basis approximation for parametrized thermoelasticity problems, *Finite Elem. Anal. Des.* 141 (2018) 96–118.